Effect of Combined Systemic and Local Morpholino Treatment on the Spinal Muscular Atrophy Δ7 Mouse Model Phenotype

Monica Nizzardo, PhD[1]; Chiara Simone, PhD[1]; Sabrina Salani, PhD[1]; Marc-David Ruepp, PhD[2]; Federica Rizzo, PhD[1]; Margherita Ruggieri, PhD[1]; Chiara Zanetta, MD[1]; Simona Brajkovic, MD[1]; Hong M. Moulton, PhD[3]; Oliver Müehlemann, PhD[2]; Nereo Bresolin, MD[1,4]; Giacomo P. Comi, MD[1]; and Stefania Corti, MD, PhD[1*]

[1]Dino Ferrari Centre, Neuroscience Section, Department of Pathophysiology and Transplantation, University of Milan, Neurology Unit, IRCCS Foundation Ca' Granda Ospedale Maggiore Policlinico, Milan, Italy; [2]Department of Chemistry and Biochemistry, University of Bern, Bern, Switzerland; [3]Biomedical Sciences, College of Veterinary Medicine, Oregon State University, Corvallis, Oregon; and [4]IRCCS Eugenio Medea, Bosisio Parini, Lecco, Italy

ABSTRACT

Background: Spinal muscular atrophy (SMA) is a fatal motor neuron disease of childhood that is caused by mutations in the *SMN1* gene. Currently, no effective treatment is available. One possible therapeutic approach is the use of antisense oligos (ASOs) to redirect the splicing of the paralogous gene *SMN2*, thus increasing functional SMN protein production. Various ASOs with different chemical properties are suitable for these applications, including a morpholino oligomer (MO) variant with a particularly excellent safety and efficacy profile.

Objective: We investigated a 25-nt MO sequence targeting the negative intronic splicing silencer (ISS-N1) 10 to 34 region.

Methods: We administered a 25-nt MO sequence against the ISS-N1 region of SMN2 (HSMN2Ex7D [-10-34]) in the SMAΔ7 mouse model and evaluated the effect and neuropathologic phenotype. We tested different concentrations (from 2 to 24 nM) and delivery protocols (intracerebroventricular injection, systemic injection, or both). We evaluated the treatment efficacy regarding SMN levels, survival, neuromuscular phenotype, and neuropathologic features.

Results: We found that a 25-nt MO sequence against the ISS-N1 region of SMN2 (HSMN2Ex7D [-10-34]) exhibited superior efficacy in transgenic SMAΔ7 mice compared with previously described sequences. In our experiments, the combination of local and systemic administration of MO (bare or conjugated to octaguanidine) was the most effective approach for increasing full-length SMN expression, leading to robust improvement in neuropathologic features and survival. Moreover, we found that several small nuclear RNAs were deregulated in SMA mice and that their levels were restored by MO treatment.

Conclusion: These results indicate that MO-mediated SMA therapy is efficacious and can result in phenotypic rescue, providing important insights for further development of ASO-based therapeutic strategies in SMA patients. (*Clin Ther.* 2014;36:340–356)
© 2014 Elsevier HS Journals, Inc. All rights reserved.

Key words: morpholino oligomer, SMAΔ7 mice, spinal muscular atrophy, survival motor neuron, therapy.

INTRODUCTION

Spinal muscular atrophy (SMA) is an autosomal recessive neuromuscular disease characterized by the degeneration of motor neurons in the spinal cord.[1] It results in progressive muscle weakness and atrophy

*Current affiliation: Department of Pathophysiology and Transplantation, University of Milan, Neurology Unit, IRCCS Foundation Ca' Granda Ospedale Maggiore Policlinico, Milan, Italy

Accepted for publication February 7, 2014.
http://dx.doi.org/10.1016/j.clinthera.2014.02.004
0149-2918/$ - see front matter

© 2014 Elsevier HS Journals, Inc. All rights reserved.

and is one of the most common genetic causes of infant mortality.[1] SMA occurs due to mutations in the *SMN1* gene, which lead to reduced SMN protein levels.[2] The SMN protein, gemins 2 to 8, and the unr-interacting protein together form the SMN complex, which is required for small nuclear ribonucleoprotein particle (snRNP) assembly and metabolism.[3–5] Spliceosomal snRNPs (U1, U2, U4, U5, U6, U11, U12, U4atac, and U6atac) combine with numerous splicing factors to form the spliceosome, which mediates the removal of introns from primary mRNA transcripts.[6,7] Thus, the SMN reduction that occurs in SMA directly affects snRNP assembly, leading to snRNPs to chiometric disequilibrium and ultimately resulting in misprocessing of certain pre-mRNAs.[8] Interestingly, this change in small nuclear RNA (snRNA) levels is cell type specific because the same snRNPs are not identically affected in all cell types.

In addition to *SMN1*, the human genome harbors the paralogous gene *SMN2*, which essentially differs from *SMN1* by a single C-to-T transition in exon 7 that modifies a splicing modulator and causes exon 7 exclusion in 90% of SMN2 mRNA transcripts.[9] The SMN protein lacking exon 7 does not oligomerize efficiently and is rapidly degraded, reducing SMN levels. The *SMN2* gene also produces 10% full-length SMN protein,[9] which is a major modulator of SMA clinical phenotype. Patients with a lower SMN2 copy number have severe SMA (type I, infantile), whereas patients with higher SMN2 copy numbers have a milder form (types III-IV, juvenile or adult onset).[9]

Currently, no effective therapies are available for SMA. Because SMA is caused by reduced SMN protein levels, most treatments have focused on increasing the amount of SMN, with strategies that include *SMN2* transcription promotion with drugs or small molecules and *SMN1* gene replacement using viral vectors carrying wild-type *SMN1*.[10] In transgenic mice with a severe SMA phenotype (SMAΔ7 mice), treatment with adenoassociated viral vectors encoding the human wild-type SMN protein results in phenotypic rescue with a log-fold increase in median survival (from weeks to more than a year).[11–14] This result is quite remarkable because this animal model has previously invariably survived no more than 2 weeks and has historically been refractory to any therapeutic attempt.[10]

An alternative promising molecular approach for SMA treatment is the modulation of SMN2 mRNA splicing to restore functional protein production.[15] Such an effect can be achieved with antisense oligos (ASOs), which are nucleotide acids analogs that can bind mRNA intronic and exonic sites and thus modify splicing events.[15] Numerous regions are involved in SMN2 splicing regulation, one of which is the negative intronic splicing silencer (ISS-N1), a 15-nucleotide splice-silencing motif located downstream of *SMN2* exon 7. ASOs targeting the ISS-N1 region promote the inclusion of exon 7 without off-target effects.[16,17] It has been hypothesized that hybridization of ASOs to the ISS-N1 region displaces trans-acting negative repressors and/or unwinds a cis-acting RNA stem-loop that interferes with the binding of U1 small nuclear RNA at the 5′ splice site of exon 7.[16,18]

Preclinical and clinical studies have examined 2 types of ASO that differ in chemical structure for use in treating human diseases through mRNA regulation: (1) the 2'-*O*-methyl-modified phosphorothioate (2OMePS) oligonucleotides or the more stable variant 2′-O-(2-methoxyethyl)-modified (MOE) phosphorothioate oligonucleotides and (2) the morpholino oligomers (MOs). In the MO ASO, the phosphorothioate-ribose backbone is replaced with a phosphorodiamidate-linked morpholine backbone that is refractory to metabolic degradation. MOs feature low toxicity and have produced encouraging results in clinical trials, such as that for Duchenne muscular dystrophy.[15] In addition, impressive phenotype rescue has been observed in mouse models of SMA after ASO-mediated SMN up-regulation in the central nervous system (CNS) using ASO-10-27 with MOE chemistry,[18] indicating promising potential as a treatment for SMA patients. The name ASO-10-27 is based on its position relative to the exon 7 donor site. Another recent work found the successful correction of SMN2 splicing with ASO-10-29 based on MO chemistry, with associated improvement of the SMA phenotype.[19]

These findings suggest that ASO-induced interference with splicing will likely be one of the first molecular therapies for SMA to reach clinical development. Indeed, ASO from ISIS Pharmaceuticals (Carlsbad, California) is already in a Phase II trial. Given their excellent safety and efficacy profile, MOs are among the most promising candidates for this purpose. However, several critical issues remain to be resolved, including the optimal type of MO chemistry and sequence and the modality of administration. It is unclear whether local injection is sufficient to rescue

SMA[19] or whether systemic injection is necessary and sufficient.[20] We have previously explored the use and optimization of MOs toward an effective clinical application, examining this strategy at the preclinical level in SMA animal models. We tested both unmodified MOs (bare MO) and octaguanidine-conjugated MOs (Vivo-MOs), which include a group of guanidinium moieties that enables systemic administration and splicing modification in adult animals.[21] The optimal MO sequence is usually approximately 25 nt; longer sequences have been used for other applications (www.gene-tools.com), but they are more costly to manufacture.

In the present study, we investigated a 25-nt MO sequence targeting the ISS-N1(-10-34) region. We compared the efficacies of bare and Vivo-MOs and of using different combinations of local and systemic administration. We found the rescue of disease phenotype in SMA mice with combined systemic and local administration during the early disease phases. In our experiments, the 25-nt MO (both bare MO and Vivo-MO) was superior to the previously described MO-10-29 and ASO-10-27 sequences.[17–20] Vivo-MO and bare MO molecules were equally effective at low doses; however, toxicity of Vivo-MO in neonatal mice limited its use at higher doses.

In the meantime and independently from our work, Zhou et al[22] performed experiments using a different mouse model ($[SMN2]_2^{+/-}$; $smn^{-/-}$) and also found that this 25-nt MO sequence was superior to other ASOs/MO sequences; however, their analyses were limited to survival and SMN expression data. Consistent with our observation, they also found that Vivo-MO is toxic in small pups. Furthermore, Mitrpant et al[23] confirmed that increased oligonucleotide length can enhance AO efficiency in promoting full-length SMN production. They designed and tested 14 different MOs of varying sizes (20, 22, and 25 nt) near ISS-N1 (-10-25), and they identified the 25-nt sequence as being the most efficacious, both in vitro and in vivo, in the SMAΔ7 mouse model. With respect to their data, our present results not only confirmed that bare 25-nt MO is the best molecule but also proved that both systemic and local injections are necessary to rescue the disease phenotype in SMA. This finding was documented by phenotypic, neuropathologic, behavioral, motor function, and molecular tests. Moreover, we found that snRNA expression levels were deregulated in SMA mice and that MO treatment restored them. Overall, our presented strategy confirmed the excellent efficacy and therapeutic potential of MOs in SMA mice.

MATERIALS AND METHODS

Morpholino Oligomers

The MO sequence was GTAAGATTCACTTTCATAATGCTGG, which was synthesized as bare MO or Vivo-MO (www.gene-tools.com). The Scr-MO sequence was GTAACATTGACTTTGATATTCCTGG, which was designed based on the best control sequence predicted using bioinformatic tool (www.gene-tools.com). MOs were dissolved in sterile saline solution at the appropriate concentration for injection (**Table 1**).

Animal Procedures

All transgenic animals were purchased from The Jackson Laboratory. All animal experiments were approved by the University of Milan and Italian Ministry of Health review boards in compliance with US National Institutes of Health guidelines.[24] Heterozygous breeding pairs ($Smn^{+/-}$, $hSMN2^{+/+}$, $SMN\Delta7^{+/+}$) were mated and genotyped as previously reported.[25] On the day of birth, SMA pups ($Smn^{-/-}$, $hSMN2^{+/+}$, $SMN\Delta7^{+/+}$) were cryoanesthetized and injected with 2 μL of MO at a predetermined concentration (**Table 1**) into the cerebral lateral ventricle, as previously described.[17,19] Briefly, the pup was cryoanesthetized and hand-mounted over a backlight to visualize the intersection of the coronal and sagittal cranial sutures. A capillary needle with injection assembly was located 1 mm lateral and 1 mm posterior to the bregma and then inserted 1 mm deep to the skin edge ipsilateral lateral ventricle.[19] Regarding bare MO, 12 nM corresponds to 101.52 μg. Subcutaneous injections in postnatal days 0 and 3 (P0 and P3) pups were performed as previously described.[20]

Western Blotting

SMN protein levels were quantified by Western blotting, as previously reported.[20] Twenty milligrams of tissue was pulverized in liquid nitrogen and homogenized in 0.4 mL (liver, kidney, or brain) or 0.2 mL (spinal cord) of 13 protein sample buffer containing 2% (wt/vol) SDS, 10% (vol/vol) glycerol, 50 mM Tris hydrochloride (pH 6.8), and 0.1 M dithiothreitol. Protein samples were separated by 12% SDS-PAGE and electroblotted onto nitrocellulose membranes. The nitrocellulose membrane was

Table 1. Outline of different treatment groups showing the injection routes and doses of MO-10–34.

Group name	Mice	No.	ICV, nM				SC, nM				Median survival	Mean survival	Mice alive	
			P0	P3	P5	P7	P0	P3	P5	P7			No.	Age
Vivo-MO														
ICV 2	SMA	3	2	2	–	–	–	–	–	–	25 d	26 d		
SC 2	SMA	4	–	–	–	–	2	2	–	–	19.5 d	18.5 d		
SC 10	SMA	3	–	–	–	–	10	10	–	–	24 d	24.6 d		
ICV and SC (Scr-MO)	SMA	3	2	–	–	–	2	2	–	–	17 d	16.5 d		
ICV and SC 2	SMA	4	2	–	–	–	2	2	–	–	42.5 d	42.5 d		
ICV and SC 2	SMA	4	–	–	2	–	–	–	2	2	26.5 d	26.5 d		
Het ICV and SC	Het	3	2	–	–	–	2	2	–	–	>17 m	>17 m		
Bare MO														
ICV 2	SMA	3	2	2	–	–	–	–	–	–	23 d	22.7 d		
ICV 24	SMA	10	24	12	–	–	–	–	–	–	1 d	10.2 d	1	58 d
SC 2	SMA	3	–	–	–	–	2	2	–	–	27 d	23.6 d		
SC 10	SMA	3	–	–	–	–	10	10	–	–	27 d	38.3 d		
SC 24	SMA	10	–	–	–	–	24	12	–	–	26 d	28.9 d	2	32 d, 32 d
ICV and SC 2	SMA	3	2	–	–	–	2	2	–	–	40 d	34.3 d		
ICV and SC 5	SMA	5	5	–	–	–	5	5	–	–	46 d	62 d		
ICV and SC 10	SMA	3	10	–	–	–	10	10	–	–	40 d	86.3 d		
ICV and SC 12	SMA	10	12	–	–	–	12	12	–	–	120 d	108.6 d	3	114 d, 51 d, 49 d
ICV and SC Scr-MO	SMA	6	10	–	–	–	10	10	–	–	17 d	17 d		
ICV and SC	SMA	5	–	–	5	–	–	–	5	5	22 d	24.8 d		
Het ICV and SC	Het	3	12	–	–	–	12	12	–	–	>17 mo	>17 mo		

Abbreviations: Bare MO = unmodified Morpholino oligomer; ICV = intracerebroventricular; Het = heterozygous; P = postnatal day; SC = subcutaneous; Scr = scrambled; SMA = spinal muscular atrophy; Vivo-MO = octaguanidine-conjugated morpholino oligomer.
The dose was referred as dose per injections.

incubated with a mouse anti-SMN monoclonal antibody, an anti-human SMN KH antibody (BD Biosciences, San Jose, California), and a rabbit anti–β-actin polyclonal antibody (Santa Cruz Biotechnology, Santa Cruz, California). Results were evaluated by chemiluminescence detection.

RNA Isolation and Quantitative Reverse Transcription–Polymerase Chain Reaction

Total RNA, including small RNAs, was isolated from tissues using the Absolutely RNA miRNA Kit (Agilent, Santa Clara, California): directly after collection of the tissues, the samples were lysed in the manufacturer's lysis buffer, homogenized using a micropestle and microtube, followed by phenol/chloroform extraction and subsequent column purification according to the manufacturer's protocol. When necessary, the eluates were additionally treated with Turbo-DNA-free (Invitrogen, Carlsbad, California) following the manufacturer's instructions. For mRNA analysis, 1 μg of total RNA was reverse transcribed in 50 μL of 1× Affinity buffer containing 10 mM dithiothreitol, 0.4 mM deoxynucleotide triphosphates, 450 ng of random hexamers, 0.4 U/μL of RiboLock (Fermentas, Hamilton, Ontario, Canada), and 1 μL of AffinityScript reverse transcriptase (Agilent) according to the manufacturer's protocol. Reverse-transcribed material corresponding to 32 ng of RNA was amplified with MESA GREEN

qPCR Master Mix Plus for SYBR (Eurogentec, Fremont, California) and the appropriate primers (600 nM each) in a total volume of 20 μL, using the Rotor-Gene 6000 rotary analyzer (Corbett Life Science, Mortlake, New South Wales, Australia)[26] (the primer sequences are listed in **Supplemental Table I** in the online version at http://dx.doi.org/10.1016/j.clinthera.2014.02.004).

Analysis of Uridylate-Rich snRNAs

For snRNA analysis, 2 μg of total RNA, including small RNAs, was reverse transcribed at 37°C in 50 μL of 1× small RNA reverse transcription buffer (10 mM Tris, pH 8, 75 mM potassium, 10 mM dithiothreitol, 70 mM magnesium chloride, 0.8 mM anchored universal reverse transcription primer, 2 U/μL of RiboLock [Fermentas], 10 mM dNTPs, and 2.5 mM random ATP) supplemented with 5 U of *Escherichia coli* Poly (A) Polymerase (New England Biolabs, Ipswitch, Massachusetts) and 1 μL of AffinityScript reverse transcriptase (Agilent). Reactions were heat inactivated for 10 minutes at 85°C.[27] Reverse-transcribed material corresponding to 18 ng of RNA was amplified with MESA GREEN qPCR Master Mix Plus for SYBR (Eurogentec) and the appropriate primers (600 nM each) in a total volume of 20 μL, using the Rotor-Gene 6000 rotary analyzer (Corbett Life Science).[27] (the primer sequences are listed in **Supplemental Table I** in the online version at http://dx.doi.org/10.1016/j.clinthera.2014.02.004).

Immunohistochemistry

Spinal cords were harvested on P9 (n = 6 animals), immersed in 4% paraformaldehyde solution and then in 20% sucrose in phosphate-buffered saline overnight, and frozen with liquid nitrogen.[19,28] The tissues were cryosectioned and mounted on gelatinized glass slides. Tissue sections were stained with anti-human SMN KH antibody (diluted 1:10) overnight and then with Alexa Fluor 594 goat anti-rabbit IgG (Molecular Probes, Eugene, Oregon) (1:1000). Motor neurons were labeled with an antibody against mouse ChAT, as previously reported.[17]

Motor Neuron Counting

Motor neuron counting was performed as previously described.[17,28] Serial cross-sections of the lumbar spinal cords were taken (12 μm thickness), and 1 of every 5 sections was processed. The number and size of all motor neurons determined in these cross-sections (n = 50 for each mouse) were quantified. We counted the cells in the spinal cord ventral horn that exhibited a fluorescent ChAT signal. To determine the mean number of motor neurons per spinal cord region for each animal, we analyzed approximately 10 levels of each spinal cord zone. Sections were taken from at least 100 μm apart to avoid double counting of the same cell. All the analyses were performed by masked investigators.

Myofiber Size

Quadriceps and intercostal skeletal muscles were fixed with paraffin and stained with hematoxylin-eosin to determine the myofiber cross-sectional size, as previously reported.[17,28] Approximately 500 myofibers were randomly chosen, and the cross-sectional area of each myofiber was measured to determine the mean myofiber size. All the analyses were performed by masked investigators.

Analysis of Neuromuscular Junctions

Analysis of neuromuscular junctions (NMJs) in selected muscles was performed as previously described.[17,28] Axons were identified by a rabbit polyclonal antibody for neurofilament medium or tubulin III (Millipore, Billerica, Massachusetts), whereas postsynaptic acetylcholine receptors were stained with Alexa 555–conjugated α-bungarotoxin (Molecular Probes). At least 100 NMJs from each muscle were randomly selected and evaluated to define the number of degenerated NMJs. All the analyses were performed by masked investigators.

Behavioral Tests

Each day, masked observers monitored all injected animals, as well as breeding pairs, for morbidity, mortality, and weight. Behavior was analyzed as previously reported.[19,20,24] The Rotarod test was performed using a 4-phase profile[20]: phase 1, from 1 to 10 rpm in 7.5 seconds; phase 2, from 10 to 0 rpm in 7.5 seconds; phase 3, from 0 to 10 rpm in 7.5 seconds in the opposite direction; and phase 4, from 10 to 0 rpm in 7.5 seconds. Hind-limb suspension tests evaluate the positioning of the legs and tail. Mice are suspended by their hind limbs from the lip of a standard 50-mL plastic centrifuge tube. The posture will be scored according to these criteria: score of 4 denotes normal hind-limb separation with tail raised; score of 3, weakness is evident and hind limbs are closer together but seldom touch each other; score of 2, hind limbs are

close to each other and often touching; score of 1, weakness is apparent and hind limbs are almost always in a clasp position with the tail raised; and score of 0, constant clasping of the hind limbs with the tail lowered. Grip-strength and righting reflex tests were performed as previously described.[29]

Statistical Analysis

Data are expressed as mean (SE). Statistical analyses were performed using 1-way ANOVA and Bonferroni multiple post hoc comparisons.[28] The Kaplan-Meier survival curve was analyzed using the log-rank test equivalent to the Mantel-Cox test.[24] All statistical analyses were performed using Stats direct software.[24] $P < .05$ was considered statistically significant. For uridylate-rich snRNA (UsnRNA) analysis, both 1-sided and unpaired t tests were performed.[27]

RESULTS

Systemic and Intrathecal Delivery of Bare and Vivo-MO Dose Dependently Rescues Transgenic Mice With Severe SMA

We designed a 25-nt MO sequence (HSMN2Ex7D [-10-34]) to target the ISS-N1 region in the *SMN2* gene based on the best bioinformatically predicted MO sequence.[30] We named this sequence MO-10-34 based on its position relative to the exon 7 donor site (Figure 1A). We synthesized both bare MO and octaguanidine-conjugated MO (Vivo-MO). We also produced a nonspecific MO with a scrambled (Scr) sequence for each MO oligomer. To determine the effectiveness of MO-10-34, we investigated different administration protocols in SMA transgenic mice that mimic type 1 severe SMA (SMA $Smn^{-/-}$, $hSMN2^{+/+}$, $SMN\Delta7^{+/+}$; called SMAΔ7 mice). Intracerebroventricular (ICV) injection of MO-10-34 bare MO and Vivo-MO on P0(Figure 1C) or subcutaneous (SC) injection on P0 and P3 (1 dose per day) (Figure 1D) (n = >3 per group) was performed using a starting dose of 2 nM, in line with previous reports,[19,20] and increasing to 24 nM. Treatment conditions and the treated SMA animal groups are described in detail in Table I. Under these conditions, we observed a significant survival increase in mice treated with bare MO or Vivo-MO using either delivery route compared with untreated and Scr-treated SMA mice. The maximum survival (72 days) was obtained with 24 nM bare MO injected ICV, which was significantly higher than that in Scr-treated mice (16 days; $P < 0.001$). However, we observed severe toxic effects for this dose, with only 2 of 10 mice surviving after the injection.

Although the observed >2-fold extension of survival was promising, it was slightly inferior to that previously reported with similar strategies. Data are controversial regarding whether SMN rescue mediated by oligonucleotide strategies necessitates intra-CNS administration, as favored by Porensky et al,[19] or systemic administration, as emphasized by Krainer et al.[20] On the basis of these considerations, we performed combined administration (ICV and SC) and increased the treatment dose. We observed dose-dependent toxicity of Vivo-MO in neonatal mice, which was in agreement with data reported by the manufacturer (Gene Tools, Philomath, Oregon) and by other groups[22] regarding local injection in young mice. This toxicity limited the possibility of further increasing the Vivo-MO dose. Injections of more than 2 nM of Vivo-MO resulted in high mortality (>50%, data not shown). Therefore, we used a range of bare MO doses (2–12 nM) and limited the Vivo-MO dose to 2 nM (Table I).

Control heterozygous mice ($Smn^{+/-}$, $hSMN2^{+/+}$, $SMN\Delta7^{+/+}$) that received ICV and SC MO-10-34 injections exhibited normal survival and behavior. SMAΔ7 mice that were untreated or injected ICV and/or SC with Scr-MO exhibited a mean survival time of 13 or 17 days, respectively (Figure 1B, 1C, and 1D). In comparison, combined ICV and SC injection of bare MO led to significant dose-dependent survival increases in SMAΔ7 mice: 2 nM, 34 days; 5 nM, 62 days; and 10 nM, 86 days (n = >3 per group; $P < 0.001$ vs Scr; Figure 1D). The maximum survival of 183 days was achieved with 10 nM bare MO. Remarkably, some of mice treated with the highest dose (12 nM) of bare MO are still alive and present complete phenotypic rescue, indicating an efficacy comparable with gene therapy (Figure 1B). The median survival obtained with 12 nM is 120 days.

Head-to-head comparison of bare MO with Vivo-MO at the same dose revealed that they were substantially equivalent regarding survival. Importantly, in our hands, 25-nt MO was superior to the previously reported MO-10-29[19] and ASO-10-27[20] sequences (see Supplemental Figure 1 in the online version at http://dx.doi.org/10.1016/j.clinthera.2014.02.004) as described by Zhou et al[22] and Mitrpant et al.[23] We also found that combined treatment in symptomatic

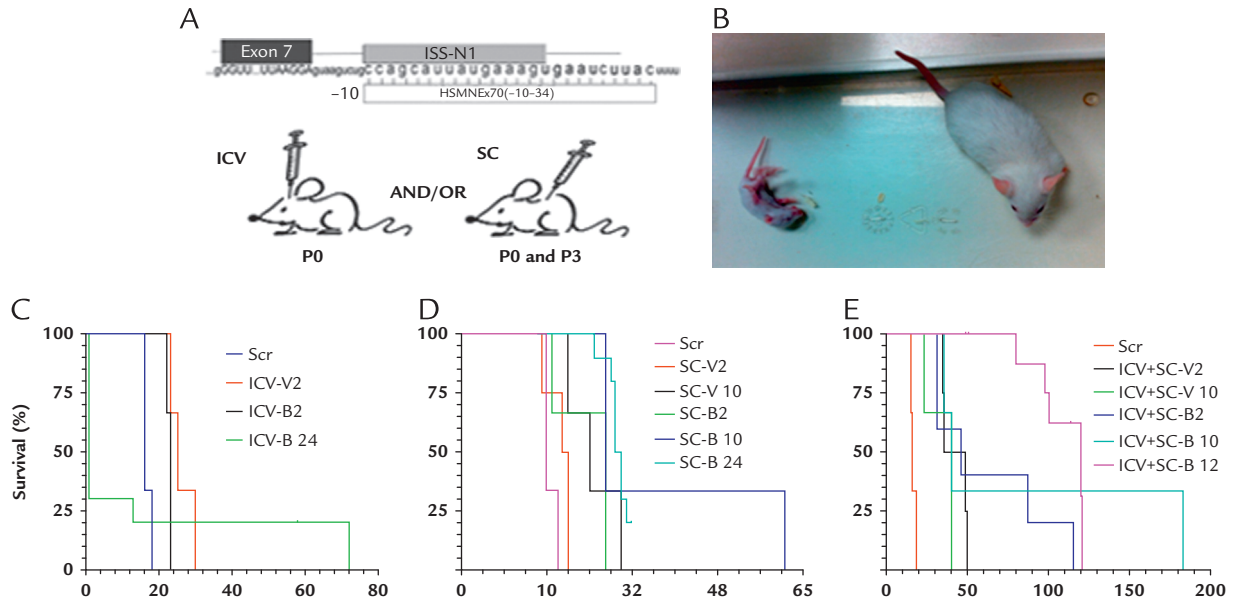

Figure 1. Morpholino oligomer (MO) 10 to 34 (MO-10-34) ameliorates the survival of spinal muscular atrophy (SMA) mice. (A) Experimental design: we designed a 25-nt MO sequence against the negative intronic splicing silencer (ISS-N1) of *SMN2* and synthesized it as unmodified MO (bare MO) or octaguanidine-conjugated MO (Vivo-MO). MO-10-34 was injected intracerebroventricularly (ICV) at postnatal day 0 (P0) and/or subcutaneously (SC) at both P0 and P3. (B) The gross appearance indicates substantial phenotypic rescue in the MO-treated SMA mice compared with the scramble (Scr)–treated (control) SMA mice. (C) Survival curves after ICV of MO-10-34 (bare MO and Vivo-MO). Administration of 2 nM MO-10-34 resulted in increased mean survival ($P < 0.001$ vs Scr-treated mice). When 24 nM MO-10-34 was administered, only 2 of 10 mice survived after the injection. (D) Survival curves after SC of MO-10-34 (bare MO and Vivo-MO). Administration of MO-10-34 SC resulted in increased mean survival ($P < 0.001$ vs Scr-treated mice) (E) Survival curves of SMA mice after combined ICV and SC administration of MO-10-34 at different concentrations (bare MO: 2–12 nM; Vivo-MO: 2 nM), which resulted in significant dose-dependent survival ($P < 0.001$ vs Scr-treated mice). B2 = mice treated with 2 nM bare MO; B10 = mice treated with 10 nM bare MO; B12 = mice treated with 12 nM bare MO; B24 = mice treated with 24 nM bare MO; V2 = mice treated with 2 nM Vivo-MO; V10 = mice treated with 10 nM Vivo-MO.

mice on P5 and P7 significantly increased survival, albeit less than early treatment (see **Supplemental Figure 1** in the online version at http://dx.doi.org/10.1016/j.clinthera.2014.02.004). This result emphasized the importance of early treatment, although protocol optimization might further improve the results after later treatment. Treated SMA mice exhibited a dose-dependent size variation from runts to mice that were comparable to their heterozygous littermates. Starting at 2 months of age, we started to detect minimal necrosis signs in the tail and ears, as well as ocular problems that were previously described as systemic signs of the SMN defect.[19,20] However, animals treated with combined ICV and SC administration of higher doses could run and climb normally (see **Supplemental Movie 1** in the online version at http://dx.doi.org/10.1016/j.clinthera.2014.02.004) and reached nearly the same appearance as heterozygous and wild-type mice, which was profoundly different from that of the Scr-treated controls that died at 2 weeks.

Effect of MO-10-34 on Exon 7 Inclusion and SMN Levels in the SMA CNS and Other Organs

To examine the molecular effect of MO on SMN levels, we subjected SMAΔ7 mice to ICV (P0) and SC (P0–P3) injection of bare MO (12 nM). MO- and Scr-treated SMA mice (n = 5 per group) were humanely

killed 7 days after treatment, as previously described in the experiments with ASO-10-27.[20] Western blots of spinal cord, brain, and liver from treated mice revealed significant increases in full-length SMN protein compared with in control mice ($P<0.001$; Figure 2C and 2D; see Supplemental Figure 2 in the online version at http://dx.doi.org/10.1016/j.clinthera.2014.02.004). Immunohistochemical staining also revealed strong SMN staining in spinal cord motor neurons from MO-treated mice (Figure 2A and 2B). These results were confirmed by quantitative reverse transcription–polymerase chain reaction of full-length human SMN2 and total SMN2 mRNA levels (n = 3 per group). Relative to Scr-treated mice, this ratio was significantly increased after MO treatment in spinal cord (8.42-fold; $P = 0.0003$), liver (17.82-fold, $P = 0.0001$), and brain (11.35-fold, $P = 0.015$) (Figure 2E) at P7. At P20, the splicing correction in the brain (1.84-fold, $P = 0.0054$) was 4.5-fold less efficient than at P7, whereas the splicing correction in the spinal cord at P20 (8.21-fold, $P = 0.045$) was comparable to that at P7 (Figure 2F). We also compared the efficiencies of splicing correction on combined 12 nM ICV and 12 nM SC vs 24 nM SC injections. The subcutaneous injection is only 2.29-fold less efficient in the brain ($P = 0.026$) and 3.26-fold less efficient in the spinal cord ($P = 0.048$) (see Supplemental Figure 3 in the online version at http://dx.doi.org/10.1016/j.clinthera.2014.02.004).

Deregulation of UsnRNA Levels in SMA7 Mice and Reduction of Deregulation by MO Treatment

Using quantitative reverse transcription–polymerase chain reaction, we investigated whether U1, U2, U4, U5, U6, U11, U12, and U4atac snRNA levels were deregulated in various tissues of SMAΔ7 mice and whether these levels were restored after MO treatment. In accordance with previous reports in other mouse models,[8] SMAΔ7 mice exhibited tissue- and snRNP-specific deregulation of all investigated UsnRNAs, except U1. We observed significantly reduced U4atac snRNA levels (by >2-fold) in the spinal cords of SMA mice treated with Scr-MO compared with heterozygous mice ($P = 0.00782$; Figure 3). Levels of the other deregulated UsnRNAs were also decreased in the spinal cords of SMA mice, except U6, which was increased. MO treatment restored the levels of all of the deregulated snRNAs to normal, including the increase of U6 snRNA (U2 snRNA $P = 0.0034$, U4 snRNA $P = 0.0049$, U5 snRNA $P = 0.0029$, U11 snRNA $P = 0.0067$, U12 snRNA $P = 0.0087$, U4atac snRNA $P = 0.0047$, and U6 snRNA $P = 0.0321$) (Figure 3). In the brains of Scr-treated SMA mice, we observed up-regulated U6 snRNA levels ($P = 0.02739$) and reductions of U4 ($P= 0.04171$) and U4atac ($P = 0.00069$) snRNA levels. MO treatment only slightly restored the deregulated snRNA levels in the brain (U2 $P = 0.08581$, U6 $P = 0.06910$, and U4atac $P = 0.05252$) (see Supplementary Figure 4 in the online version at http://dx.doi.org/10.1016/j.clinthera.2014.02.004). In the liver, we observed down-regulation of U4 ($P = 0.07705$) and U4atac ($P = 0.00685$), and the levels of U4 snRNA in the liver were fully restored by MO treatment ($P = 0.00089$; see Supplementary Figure 4 in the online version at http://dx.doi.org/10.1016/j.clinthera.2014.02.004).

Effect of MO on Motor Neuron Cell Number in the Spinal Cord and Muscle Trophism in Treated SMA Mice

To determine the efficacy of MO treatment regarding improvement of the neuropathologic phenotype, we analyzed SMAΔ7 mice treated with 12 nM bare MO by both ICV and SC compared with Scr-treated mice. We investigated spinal cord motor neuron cell counts and muscle morphology parameters in P9 mice (n = 5 per group). Histologic examination revealed striking improvements in MO-treated mice. The number of motor neurons per spinal cord in MO-treated mice was comparable to that in control heterozygous littermates and was significantly higher than in untreated animals ($P < 0.001$; see Supplemental Figure 5 in the online version at http://dx.doi.org/10.1016/j.clinthera.2014.02.004). Staining of the NMJs with α-bungarotoxin revealed that NMJ architecture in treated mice was similar to that of their heterozygous littermates, and the mean NMJ diameter was significantly increased in treated compared with untreated SMAΔ7 mice ($P < 0.001$; Figure 4). MO injection resulted in statistically significant increases in muscle growth, evaluated by quantification of the mean myofiber cross-sectional area for each group (MO-treated vs Scr-treated mice, $P < 0.001$; Figure 5). The heart weight of MO-treated mice was also similar to that of their heterozygous littermates and was significantly increased compared with in untreated SMAΔ7 animals (see Supplemental Figure 6 in the online version at http://dx.doi.org/10.1016/j.clinthera.2014.02.004).

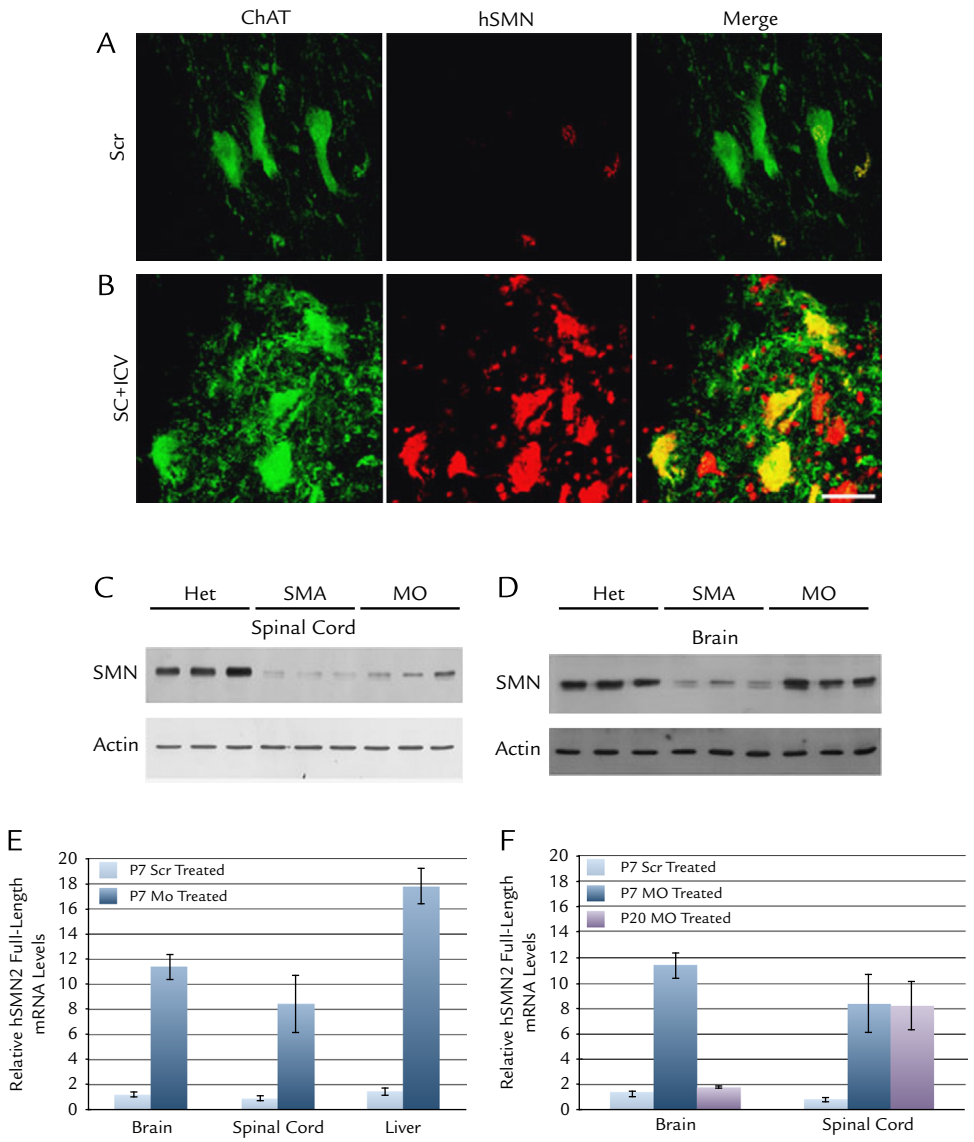

Figure 2. Morpholino oligomer (MO) 10 to 34 (MO-10-34) treatment increases SMN expression in spinal muscular atrophy (SMA) mice. Treatment with MO-10-34 increased SMN protein expression and the numbers of motor neurons in the spinal cord after intracerebroventricular (ICV) and subcutaneous (SC) injection of neonatal mice with severe SMA at postnatal day 0 (P0) and P3. (A and B) Immunohistochemical staining revealed increased SMN expression in spinal cord motor neurons at 7 days after MO treatment. ChAT, green; SMN, red. (C and D) Seven days after treatment, Western blotting was used to evaluate the amounts of SMN protein in the spinal cords and brains of MO-10-34–treated mice relative to scramble (Scr)–treated and wild-type mice, indicating significant increases in SMN ($P < 0.001$). (E) After MO treatment, human SMN2 (hSMN2) full-length mRNA levels (relative to Scr-treated samples and normalized to 5.8S rRNA) increased in brain (11.35-fold, $P = 0.015$), spinal cord (8.42-fold; $P = 0.0003$), and liver (17.82-fold, $P = 0.0001$). Data are presented as mean (SEM). (F) hSMN2 full-length mRNA levels at P7 and P20, relative to the corresponding Scr-treated samples and normalized to 5.8S rRNA. At P20, the splicing correction in the brain (1.84-fold; $P = 0.0054$) was 4.5-fold less efficient as at P7, whereas the splicing correction in spinal cord (8.21-fold; $P = 0.045$) was comparable between P20 and P7. Data are presented as mean (SEM). HET = heterozygous mice.

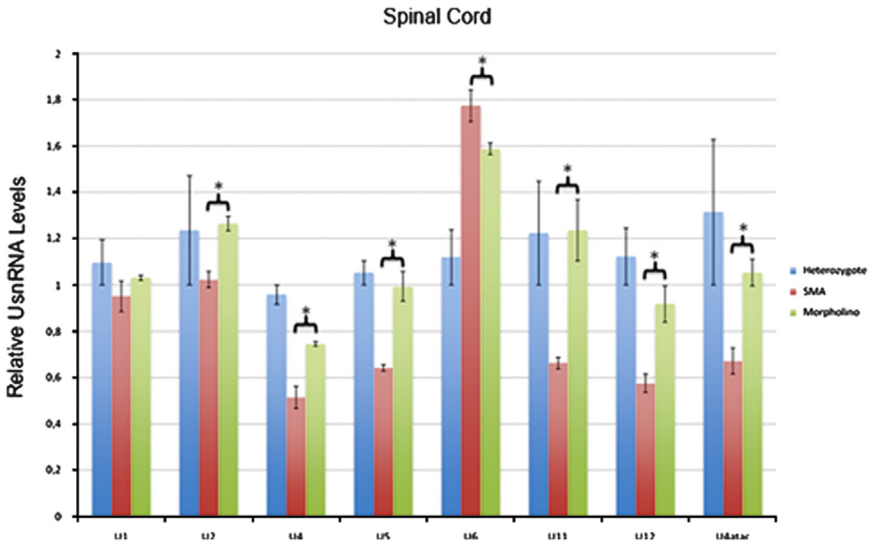

Figure 3. Morpholino oligomer (MO) 10 to 34 (M0-10-34) treatment restores the expression levels of deregulated small nuclear RNAs (snRNAs) in spinal muscular atrophy (SMA) mice. SMA mice exhibited deregulated snRNA expression levels in the spinal cords, which were partially restored after MO treatment. Data are presented as mean (SEM). The uridylate-rich snRNA (UsnRNA) levels are normalized to 7SL-RNA and set relative to the levels in heterozygous (Het) mice. *$P < 0.05$.

Effect of MO on Neuromuscular Function in SMA Mice

In proportion to the amelioration observed in motor neuron count and muscle physiology, most of the mice that were treated with the combined ICV and SC injections of higher MO doses exhibited no overt signs of motor dysfunction and were almost indistinguishable from their heterozygous littermates (see **Supplemental Movie 1** in the online version at http://dx.doi.org/10.1016/j.clinthera.2014.02.004; **Figure 6**). We used different tests to evaluate behavior and motor function during the first weeks of life (when Scr-treated mice were still alive) and during adulthood. In the early stages, we evaluated the mice using the righting test, test tube score, hand grip test, and weight. In each test, treated animals dose dependently performed significantly better than untreated and Scr-treated SMA mice ($P < 0.001$ vs Scr-treated mice).

At 3 months of age, mice were subjected to the Rotarod test, which requires limb muscle strength, balance, and coordination. Three-month-old MO-treated SMA mice were able to stay on the rotating rod for the same amount of time as control heterozygotes. Many treated mice, as well as the heterozygotes, passed a 30-second acceleration-profile test (**Figure 6J and 6K**; see **Supplemental Movie 2** in the online version at http://dx.doi.org/10.1016/j.clinthera.2014.02.004). Because SMA is a neuromuscular disease, this performance is remarkable proof of phenotypic amelioration. At this stage, the treated SMA mice were able to walk, explore the environment, and perform various behaviors similarly to control heterozygous mice (**Figure 6**). Overall, these results combined with the above-presented survival data support a complete rescue of SMA phenotype in this animal model treated with the combined injections.

DISCUSSION

Modulating RNA splicing to restore functional protein production is one of the most promising therapeutic options to treat neuromuscular diseases, including SMA. Because *SMN2* can produce a small amount of full-length SMN protein by alternative splicing, one possible strategy is to target *SMN2* to increase SMN production in patients with SMA. Recent developments in ASO technology include

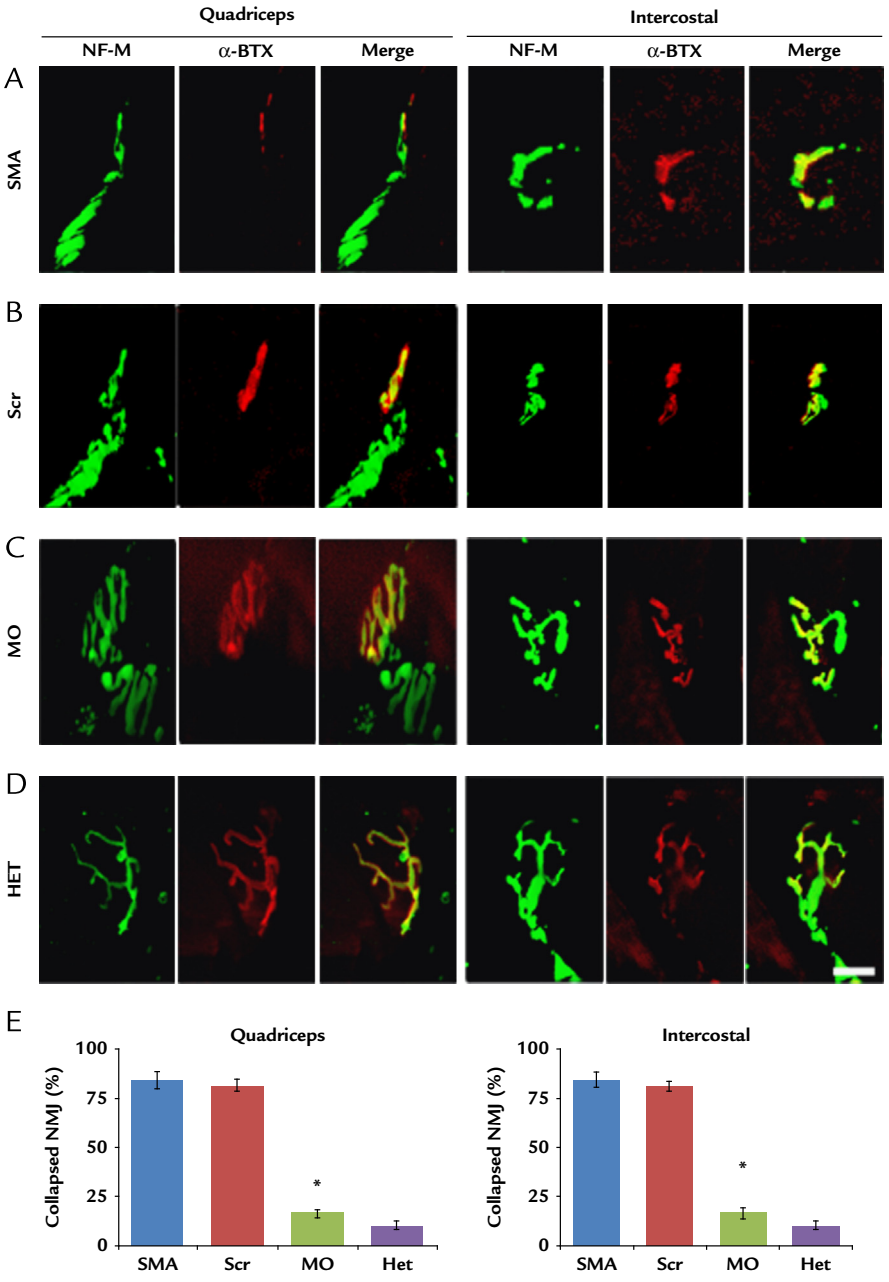

Figure 4. Morpholino oligomer (MO) 10 to 34 (MO-10-34) treatment ameliorates neuromuscular junction (NMJ) structure in spinal muscular atrophy (SMA) mice. NMJ staining of muscle fibers from the quadriceps (left) and intercostal (right) muscles of untreated SMA mice (A), scramble (Scr)–treated SMA mice (B), MO-10-34–treated SMA mice (C), and untreated heterozygous (Het) mice (D) at 9 days. The axons of presynaptic motor neurons were stained with antibody raised against neurofilament medium (NF-M) (green). The acetylcholine receptors of the postsynaptic termini were labeled with α-bungarotoxin (α-BTX; red). The overlay of both signals (yellow) indicates innervation at the motor end-plate. In untreated and Scr-treated SMA mice, the presynaptic termini present a collapsed structure, suggesting a pathologic NMJ. (E) The percentage of NMJs exhibiting a collapsed feature was determined at 9 days. *P* values between different treatment groups were determined using 1-way ANOVA and Bonferroni multiple post hoc comparisons ($P < 0.001$). Data are presented as mean (SEM). Scale bar = 10 μm.

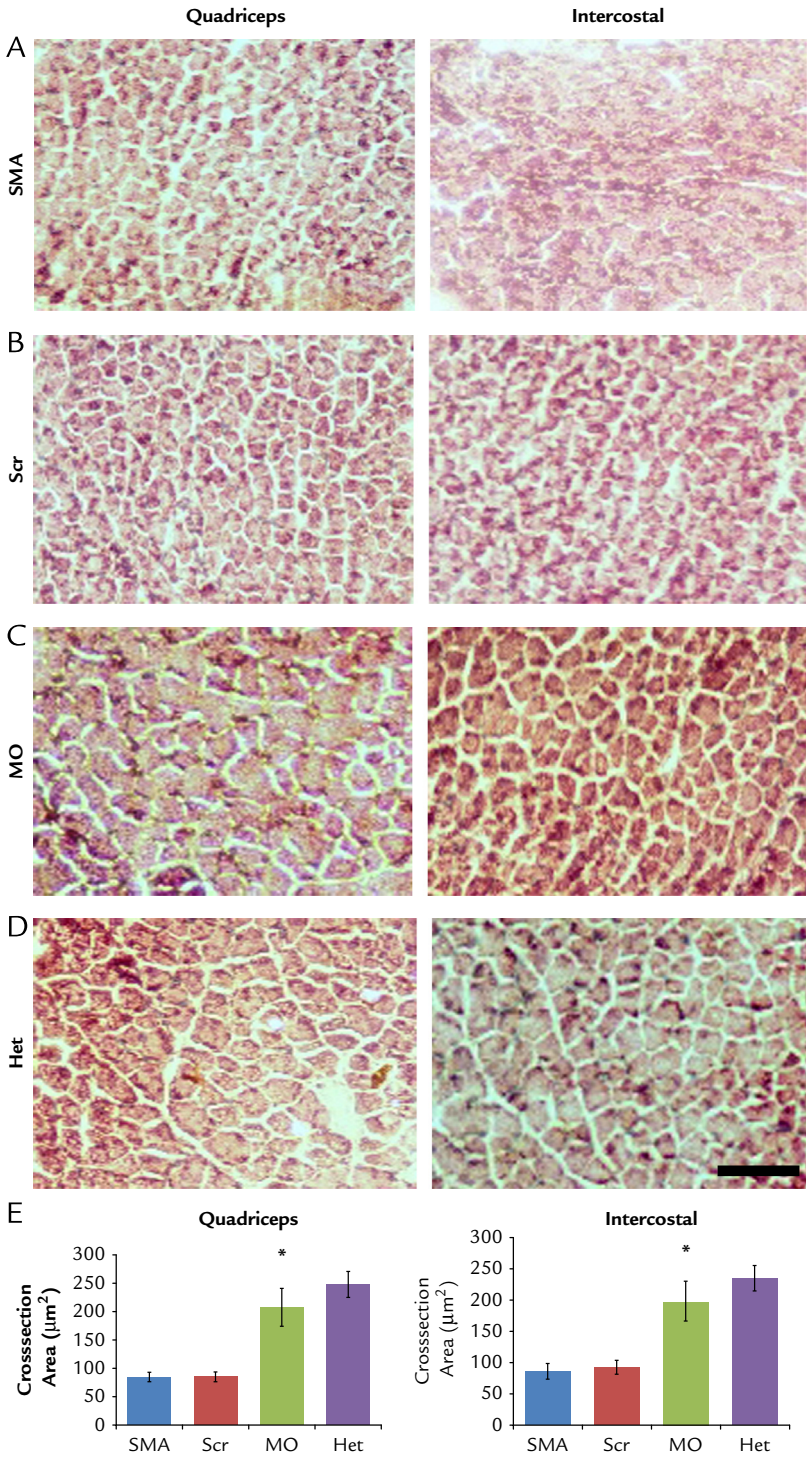

Figure 5. Morpholino oligomer (MO) 10 to 34 (MO-10-34) treatment improves muscle trophism in spinal muscular atrophy (SMA) mice. Hematoxylin-eosin staining of the quadriceps (left) and intercostal (right) muscles of untreated SMA mice (A), scramble (Scr)–treated SMA mice (B), MO-10-34–treated SMA mice (C), and untreated heterozygous (Het) mice (D) at 9 days. (E) The mean myofiber cross-sectional area for each group was quantified. *P* values between different treatment groups were determined using 1-way ANOVA and Bonferroni multiple post hoc comparisons ($P < 0.001$). Data are presented as mean (SEM). Scale bar = 100 μm.

2OMePS and the MOE variant. MOs have produced encouraging results in animal models of neuromuscular disorders and more recently in clinical trials, including the targeted skipping of exon 51 in Duchenne muscular dystrophy.[15] This technology has made it possible for us and others to restore SMN expression in SMA mice, in many cases achieving complete phenotype rescue.[17,19,20,22,23]

Both phosphorothioate ASO and MO chemistries are promising for treating neuromuscular diseases, but bare MO has been found to be superior to 2OMePS molecules in some experimental models (particularly in Duchenne muscular dystrophy animal models) because of its stability and efficacy in targeting mRNA[15] and its excellent safety profile. It was previously reported that 2OMe-based ASOs did not perform adequately in vivo in SMA animals,[31] whereas MOE chemistry was active and well tolerated, with impressive results in SMA mice.[20] Our current results confirm and extend the previous data indicating the excellent efficacy of MO in redirecting SMN2 splicing and thus improving the SMA disease phenotype at the molecular, cellular, and functional levels in a mouse model of severe SMA type 1 disease.

In agreement with previous studies, we found that combined subcutaneous and local injection of bare MO and Vivo-MO successfully modified SMN2 splicing, resulting in robust expression of SMN mRNA and protein. In turn, this SMN up-regulation correlated with increased numbers of motor neurons, amelioration of NMJ architecture, and improved muscle trophism, which led to impressive therapeutic effects in SMA mice in terms of survival and neuromuscular function. The phenotype of some SMA animals treated with the higher dose was almost indistinguishable from their heterozygous littermates.

The successful translation of this strategy into clinical use will rely on the continued optimization of this approach, which was one goal of our work. Some critical points in the development of this technique include the design of the best MO oligomer sequence and the investigations of various chemical modifications. We evaluated a 25-nt sequence that was predicted to be the best sequence by an algorithm from Gene Tools. We found that it indicated a higher efficacy than was previously described for ASO-10-27 and ASO-10-29 synthesized with MO chemistry,[17,19,20] as was also found by the groups of Zhou et al[22] and Mitrpant et al.[23] We cannot directly compare ASO-10-27 synthesized as MOE with our MO-10-34 sequence because of the patent on MOE chemistry (ISIS Pharmaceuticals). Overall, our data confirm the critical importance of targeting the ISS-N1 region for effective modulation of SMN2 splicing and emphasize that small variations in the ASO sequences used can be important.

Regarding the chemical modification of oligomers, we tested Vivo-MO molecules that have a terminal octaguanidinium dendrimer to enhance cell permeability. Vivo-MOs have been previously described as superior to nonconjugated MO for achieving mRNA targeting after intravenous administration in animals.[21] We found that Vivo-MO improved the SMA phenotype equally to, but not better than, bare MO. One possible explanation for this finding is that MOs were administered in neonatal mice, which have more permeable tissues and cells, allowing the bare MO to more easily enter the cytoplasm. Furthermore, as previously described by the manufacturer (Gene Tools), we found that neonatal mice did not tolerate high doses of Vivo-MO, and we were thus unable to further increase the dose. The described toxicity was also in accordance with the findings of Zhou et al.[22] Although administration of Vivo-MO may be more advantageous than bare MO during the symptomatic phase, this potential benefit could not be entirely appreciated because it is more difficult to modify disease progression at this stage. It would be interesting in future studies to evaluate local injection of bare MO in conjunction with systemic administration of Vivo-MO in presymptomatic and symptomatic phases.

Remarkably, we observed significant phenotypic amelioration during symptomatic phases, which warrants additional investigation with alternative protocols. Addressing the disease after its onset is a present challenge in SMA research. For this purpose, it will be necessary to better understand the pathogenetic mechanisms responsible for disease progression even when SMN expression is restored. We hypothesize that the best therapy will be a combination of molecular therapies that address SMN level in addition to other later pathogenetic events.

The ideal route of administration of antisense oligonucleotides remains an open and controversial issue. Although 2 other groups have evaluated both routes of administration, the conclusions of Hua et al[20] emphasized the importance of peripheral administration, whereas Porensky et al[19] highlighted that local CNS administration is crucial. Both groups

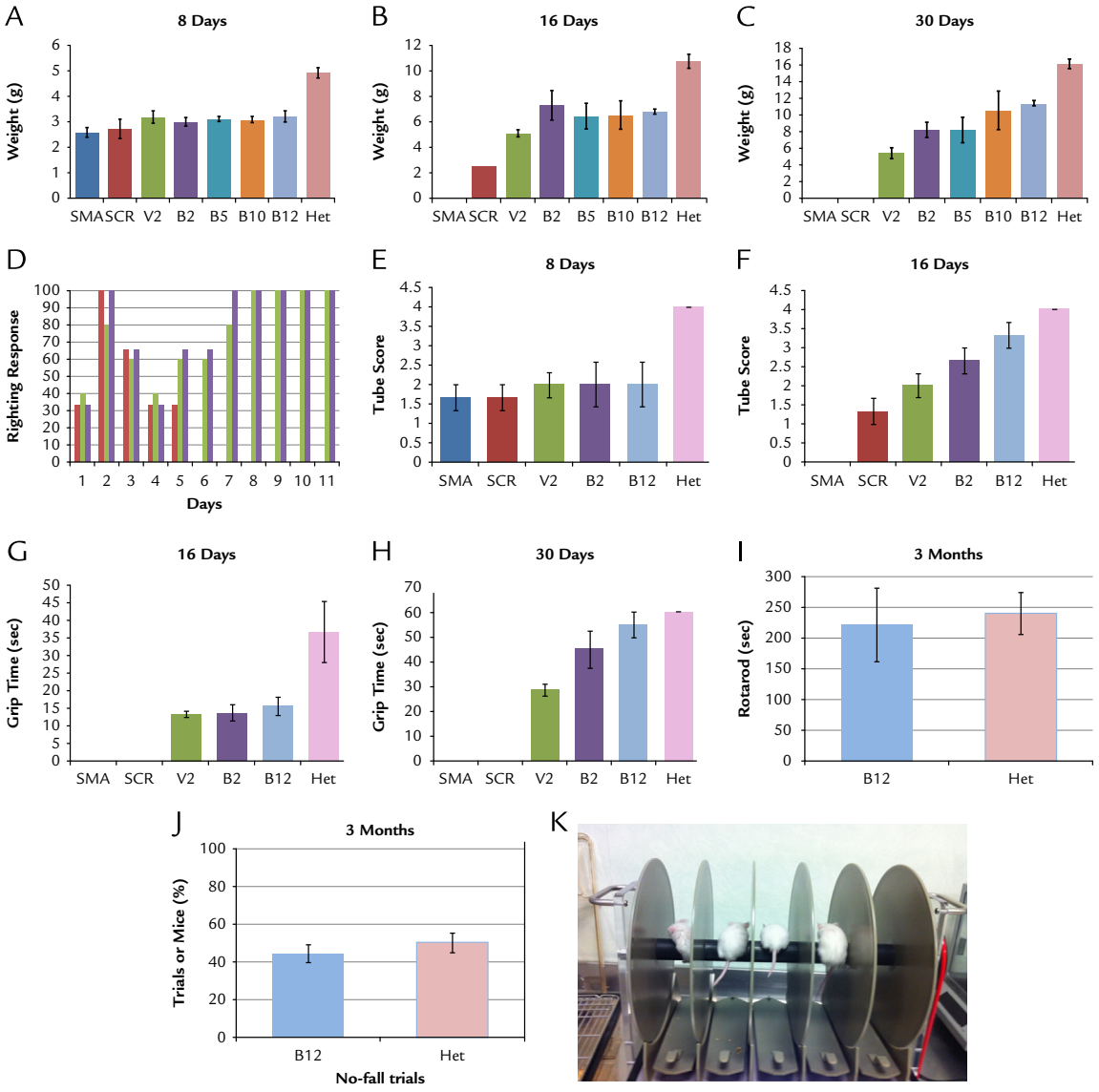

Figure 6. Morpholino oligomer (MO) 10 to 34 (MO-10-34) treatment ameliorates the phenotype and neuromuscular function of spinal muscular atrophy (SMA) mice. Weights at 8 (A), 16 (B), and 30 days (C) indicate significant dose-dependent weight increases in treated mice compared with untreated and scramble (Scr)–treated SMA mice at 16 and 30 days ($P < 0.001$). (D) The righting reflex was significantly improved in MO-treated mice beginning at day 5 ($P < 0.001$ compared with untreated and Scr-treated SMA mice). Tube score (E and F) and grip time (G and H) were also significantly improved by treatment, beginning at day 16 ($P < 0.001$). The neuromuscular performance of MO-treated mice (12 nM) was tested using a Rotarod with an acceleration profile. The mean times for staying on the spinning rod (I) and the percentages of no-fall trials and of mice with a no-fall trial (J) are shown. Treated mice performed as well as heterozygous (Het) mice. *P* values between different treatment groups were determined using 1-way ANOVA and Bonferroni multiple post hoc comparisons. Data are mean (SEM). (K) The SMA mice treated with 12 nM MO were able to perform the Rotarod test. B2 = mice treated with 2 nM unmodified MO (bare MO); B5 = mice treated with 5 nM bare MO; B10 = mice treated with 10 nM bare MO; B12 = mice treated with 12 nM bare MO; V2 = mice treated with 2 nM octaguanidine-conjugated MO.

tested the combinatory strategy but only in a small subset of experiments. Hua et al[20] found that a combined injection protocol resulted in a major improvement of median survival compared with ICV alone, but their best results were obtained with a SC injection at a high dose. Porensky et al[19] also used the combinatory administration and found that it produced an impressive survival advantage that was equivalent to, but not greater than, high-dose MO injected ICV at P0.

In addition, our data indicate that the combined regimen at the maximal tested dose was more efficacious compared with use of a single route, even if the combined administration yielded the same survival rate as reported previously for ICV administration alone. We produced a new set of data that allow for better comparison between ICV and SC single-route administration compared with combinatorial administration at higher doses. The highest dose injected only SC resulted in a modest survival increase to a mean of 28.8 days, with 2 mice remaining alive at 32 days, which was much lower than the survival achieved with the combined injection of the same dose. For ICV administration of the same dose, we observed severe toxic effects, and the mice that were not killed by the injection exhibited shorter survival than did all of the mice treated with combined injections. This adverse effect was not linked to a problem associated with the volume of the injection but to the high dose given in a single administration. For example, Porensky et al injected 135 μg of ICV MO per injection at P0, P1, and P2 for a total of 405 μg with no signs of toxic effects.

An analysis of SMN2 splicing modulation achieved by the same dose (24 nM) using different administration regimens revealed that splicing in the CNS was less effective with SC injection only than with the combined administration protocol (12 nM ICV and 12 nM SC), suggesting that the systemic injection of MO results in limited diffusion in the CNS and likely has a therapeutic effect on the peripheral organs (see **Supplemental Figure 3** in the online version at http://dx.doi.org/10.1016/j.clinthera.2014.02.004), even if the blood brain barrier is partially open for MO when the injections are given. These findings support the hypothesis that the peripheral actions of MO may have a role in phenotype rescue because the full phenotype rescue could not be entirely accounted for by CNS action alone. Overall, at the maximal tested dose, the combined regimen was the most efficacious method. We believe that our findings provide a new, more balanced perspective regarding the antisense effect on SMA rescue.

SMN deficiency affects snRNPs in a tissue- and subset-specific manner.[8,32] The snRNPs that are most affected by SMN depletion are the so-called minor snRNPs that constitute the minor spliceosome. Although most introns in pre-mRNAs are processed by the major spliceosome (composed of U1, U2, U4/U6, and U5 snRNPs), approximately 1% of introns require the activity of the minor spliceosome (composed of U11, U12, U4atac/U6atac, and U5 snRNPs).[33,34] Importantly, several genes required for motor circuit function are dependent on the minor spliceosome for proper pre-mRNA splicing.[35] We observed that almost all of the analyzed snRNAs were deregulated in SMA mice, with the minor snRNA U4atac being most affected by SMN deficiency in all tissues, along with its major spliceosome counterpart U4. Importantly, MO treatment of SMAΔ7 mice fully restored snRNA levels in the spinal cord to those present in healthy heterozygous mice. This analysis provides deeper insights into the pathogenetic mechanism. It will be of great interest to study the dose-dependent effects of MO on the restoration of the individual snRNA levels and to validate whether the detection of snRNAs levels in peripheral blood can be used as a diagnostic marker and for therapy assessment.

The remarkable and reproducible efficacy of MO regarding life extension, gains of weight and strength, and neuropathologic feature improvement is comparable to that obtained with gene therapy. MOs have a notably excellent safety profile, which has already been tested in clinical trials. Importantly, the gene stays expressed under its own endogenous promoter, subjected to its regular turnover, thus obviating the need for transgene introduction. Disadvantages of ASO therapy for SMA include the likelihood of relatively invasive repeat CNS dosing; however, this disadvantage can be overcome with the aid of the electronic pump that is already used to administer the drug intrathecally in the clinic.[36,37] Indeed, we believe that systemic administration must be associated with local delivery. Ideally, if the chemical modification of ASOs or their conjugation with peptide will allow efficient crossing of the blood brain barrier, then systemic noninvasive administration will likely be

the better option. For instance, it has been previously reported that 9 arginine tags fused to rabies virus glycoprotein peptides can deliver antisense oligonucleotides across the blood brain barrier.[38]

Overall, in the present study, we achieved our primary objectives of correcting SMA phenotypes in mice using MO and expanding the knowledge of the field regarding selection of the best oligomer sequence, MO chemistry, dose-response effect, and route of administration. Future studies are needed to pursue continued improvement of the administration protocol (time, dose, and route of administration) and should include tests in other larger animal models to confirm the data obtained in mice and to progress toward future clinical trials. MO has the potential to ameliorate the natural history of SMA and requires further evaluation in clinical safety and efficacy profile trials.

ACKNOWLEDGMENT

The authors would like to thank the Associazione Amici del Centro Dino Ferrari for their support, the Swiss National Science Foundation (CRSII3-136222), and the NOMIS Foundation for supporting Marc-David Ruepp.

Drs. Nizzardo and Simone performed all in vivo experiments. Dr. Zanetta performed the in vivo functional analysis. Dr. Salani performed the western blot analysis. Drs. Ruepp and Brajkovic performed the molecular biology experiments. Drs. Rizzo and Ruggieri performed the hystopatological analysis. Drs. Bresolin, Moulton and Muehlemann participated in the revision of the manuscript. Dr. Comi contributed ideas and supported the work. Drs. Corti and Nizzardo conceived the experiments and wrote the manuscript. Dr. Simone contributed to writing the manuscript.

CONFLICTS OF INTEREST

The authors have no financial conflicts of interest to declare.

FUNDING SOURCES

This work was supported by grant GGP09107 from the Telethon Foundation and grant RBFR08RV86 from the Ministry of Instruction, University and Research.

SUPPLEMENTARY MATERIAL

Supplementary material cited in this article is available online at http://dx.doi.org/10.1016/j.clinthera.2014.02.004.

REFERENCES

1. D'Amico A, Mercuri E, Tiziano FD, Bertini E. Spinal muscular atrophy. *Orphanet J Rare Dis*. 2011;2:6–71.
2. Lefebvre S, Bürglen L, Reboullet S, et al. Identification and characterization of a spinal muscular atrophy-determining gene. *Cell*. 1995;80:155–165.
3. Kolb SJ, Battle DJ, Dreyfuss G. Molecular functions of the SMN complex. *J Child Neurol*. 2007;8:990–994.
4. Cauchi RJ. SMN and Gemins: 'we are family' ... or are we? insights into the partnership between Gemins and the spinal muscular atrophy disease protein SMN. *Bioessays*. 2010;32:1077–1089.
5. Battle DJ, Kasim M, Yong J, et al. The SMN complex: an assembly machine for RNPs. *Cold Spring Harb Symp Quant Biol*. 2006;71:313–320.
6. Will CL, Lührmann R. Spliceosomal UsnRNP biogenesis, structure and function. *Curr Opin Cell Biol*. 2001;13:290–301.
7. Nilsen TW. The spliceosome: the most complex macromolecular machine in the cell? *Bioessays*. 2003;25:1147–1149.
8. Zhang Z, Lotti F, Dittmar K, Younis I, Wan L, Kasim M, Dreyfuss G. SMN deficiency causes tissue-specific perturbations in the repertoire of snRNAs and widespread defects in splicing. *Cell*. 2008;133:585–600.
9. Lorson CL, Strasswimmer J, Yao JM, et al. SMN oligomerization defect correlates with spinal muscular atrophy severity. *Nat Genet*. 1998;19:63–66.
10. Lewelt A, Newcomb TM, Swoboda KJ. New therapeutic approaches to spinal muscular atrophy. *Curr Neurol Neurosci Rep*. 2012;12:42–53.
11. Foust KD, Wang X, McGovern VL, et al. Rescue of the spinal muscular atrophy phenotype in a mouse model by early postnatal delivery of SMN. *Nat Biotechnol*. 2010;28:271–274.
12. Passini MA, Bu J, Roskelley EM, et al. CNS-targeted gene therapy improves survival and motor function in a mouse model of spinal muscular atrophy. *J Clin Invest*. 2010;120:1253–1264.
13. Valori CF, Ning K, Wyles M, et al. Systemic delivery of scAAV9 expressing SMN prolongs survival in a model of spinal muscular atrophy. *Sci Transl Med*. 2010;2:35–42.
14. Dominguez E, Marais T, Chatauret N, et al. Intravenous scAAV9 delivery of a codon-optimized SMN1 sequence rescues SMA mice. *Hum Mol Genet*. 2010;20:681–693.
15. Muntoni F, Wood MJ. Targeting RNA to treat neuromuscular disease. *Nat Rev Drug Discov*. 2011;10:621–637.
16. Singh NN, Singh RN, Androphy EJ. Modulating role of RNA structure in alternative splicing of a critical exon in the

spinal muscular atrophy genes. *Nucleic Acids Res*. 2007;35:371–389.
17. Passini MA, Bu J, Richards AM, et al. Antisense oligonucleotides delivered to the mouse CNS ameliorate symptoms of severe spinal muscular atrophy. *Sci Transl Med*. 2011;3:72ra18.
18. Hua Y, Vickers TA, Okunola HL, Bennett CF, Krainer AR. Antisense masking of an hnRNP A1/A2 intronic splicing silencer corrects SMN2 splicing in transgenic mice. *Am J Hum Genet*. 2008;82:834–848.
19. Porensky PN, Mitrpant C, McGovern VL, et al. A single administration of morpholino antisense oligomer rescues spinal muscular atrophy in mouse. *Hum Mol Genet*. 2012;21:1625–1638.
20. Hua Y, Sahashi K, Rigo F, et al. Peripheral SMN restoration is essential for long-term rescue of a severe spinal muscular atrophy mouse model. *Nature*. 2011;478:123–126.
21. Parra MK, Gee S, Mohandas N, Conboy JG. Efficient in vivo manipulation of alternative pre-mRNA splicing events using antisense morpholinos in mice. *J Biol Chem*. 2011;286:6033–6039.
22. Zhou H, Janghra N, Mitrpant C, Dickinson R, Anthony K, Price L. A novel morpholino oligomer targeting ISS-N1 improves rescue of severe SMA transgenic mice. *Hum Gene Ther*. 2013;24:331–342.
23. Mitrpant C, Porensky P, Zhou H, et al. Improved antisense oligonucleotide design to suppress aberrant SMN2 gene transcript processing: towards a treatment for spinal muscular atrophy. *PLoS One*. 2013;8:e62114.
24. Corti S, Nizzardo M, Nardini M, et al. Embryonic stem cell-derived neural stem cells improve spinal muscular atrophy phenotype in mice. *Brain*. 2010;133:465–481.
25. Le TT, Pham LT, Butchbach ME, Zhang HL. SMNDelta7, the major product of the centromeric survival motor neuron (SMN2) gene, extends survival in mice with spinal muscular atrophy and associates with full-length SMN. *Hum Mol Genet*. 2005;14:845–857.
26. Ruggiu M, McGovern VL, Lotti F, Saieva L, Li DK, Kariya S. A role for SMN exon 7 splicing in the selective vulnerability of motor neurons in spinal muscular atrophy. *Mol Cell Biol*. 2012;32:126–138.
27. Ruepp MD, Vivarelli S, Pillai RS, et al. The 68 kDa subunit of mammalian cleavage factor I interacts with the U7 small nuclear ribonucleoprotein and participates in 3'-end processing of animal histone mRNAs. *Nucleic Acids Res*. 2010;38:7637–7650.
28. Corti S, Nizzardo M, Simone C, et al. Genetic correction of human induced pluripotent stem cells from patients with spinal muscular atrophy. *Sci Transl Med*. 2012;4. 165–162.
29. Grondard C, Biondi O, Armand AS, et al. Regular exercise prolongs survival in a type 2 spinal muscular atrophy model mouse. *J Neurosci*. 2005;25:7615–7622.
30. Morcos PA. Achieving targeted and quantifiable alteration of mRNA splicing with Morpholino oligos. *Biochem Biophys Res Commun*. 2007;358:521–527.
31. Williams JH, Schray RC, Patterson CA, Ayitey SO, Tallent MK. Oligonucleotide-mediated survival of motor neuron protein expression in CNS improves phenotype in a mouse model of spinal muscular atrophy. *J Neurosci*. 2009;29:7633–7638.
32. Gabanella F, Butchbach ME, Saieva L, Carissimi C, Burghes AH, Pellizzoni L. Ribonucleoprotein assembly defects correlate with spinal muscular atrophy severity and preferentially affect a subset of spliceosomal snRNPs. *PLoS One*. 2007;2:e921.
33. Patel AA, Steitz JA. Splicing double: insights from the second spliceosome. *Nat Rev Mol Cell Biol*. 2003;4:960–970.
34. Levine A, Durbin R. A computational scan for U12-dependent introns in the human genome sequence. *Nucleic Acids Res*. 2001;29:4006–4013.
35. Lotti F, Imlach WL, Saieva L, et al. An SMN-dependent U12 splicing event essential for motor circuit function. *Cell*. 2012;151:440–454.
36. Slavin KV, Hsu FPK, Fessler RG. Intrathecal opioids: intrathecal drug-delivery systems. In: Burchiel KJ, ed. *Surgical Management of Pain*.. New York, NY: Thieme; 2002:603–613.
37. Smith TJ, Staats PS, Deer T, et al. Randomized clinical trial of an implantable drug delivery system compared with comprehensive medical management for refractory cancer pain: impact on pain, drug-related toxicity, and survival. *J Clin Oncol*. 2002;20:4040–4049.
38. Kumar P, Wu H, McBride JL, Jung KE, Kim MH, Davidson BL. Transvascular delivery of small interfering RNA to the central nervous system. *Nature*. 2007;448:39–43.

Address correspondence to: Stefania Corti, Department of Pathophysiology and Transplantation, University of Milan, Neurology Unit, IRCCS Foundation Ca' Granda Ospedale Maggiore Policlinico, Via F. Sforza 35, 20122 Milan, Italy. E-mail: stefania.corti@unimi.it

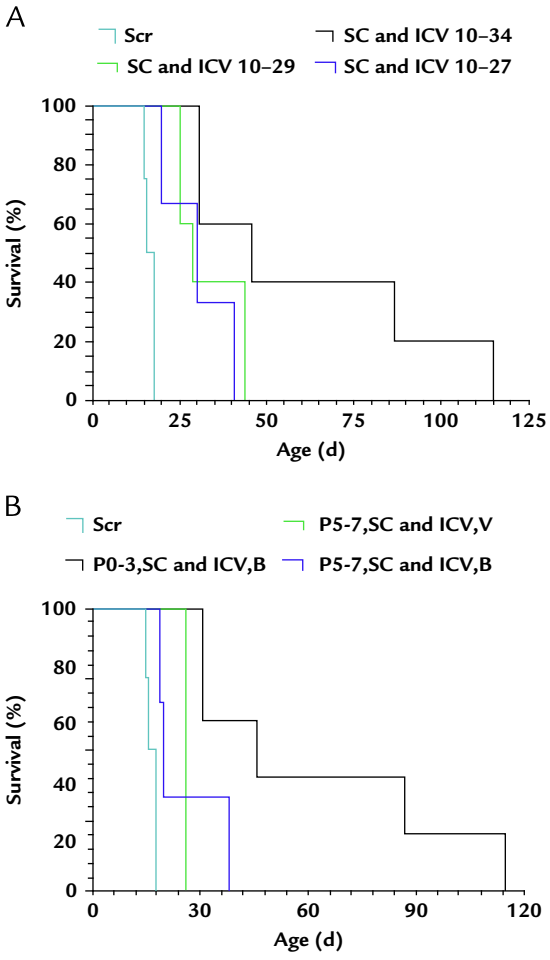

Supplemental Figure 1. Morpholino oligomer (MO) 10 to 34 (MO-10-34) increased survival of spinal muscular atrophy (SMA) mice more than MO-10-29 or antisense oligo 10 to 27 (ASO-10-27) and exerted a positive effect during the symptomatic phase. (A) Survival curves of SMA mice after combined intracerebroventricular (ICV) at postnatal day 0 (P0) and subcutaneous (SC) at P0 and P3 administration of MO-10-34, ASO-10-27, and MO-10-29 (5 nM). Scramble (Scr)–treated mice served as controls. A significant increase in survival was observed in mice treated with MO-10-34 compared with the other 2 sequences ($P < 0.001$ vs MO-10-29, ASO-10-27, and Scr). (B) Survival curves of SMA mice after combined ICV (P0) and SC (P0 and P3) of unmodified MO (bare MO) or ICV (P5) and SC (P5 and P7) administration of MO-10-34 (bare MO or octaguanidine-conjugated MO). Dose was 5 nM. Scr-treated mice served as controls. A significant increase in survival was observed in early treatment compared with late administration ($P < 0.001$ vs P5 and P7 treatment).

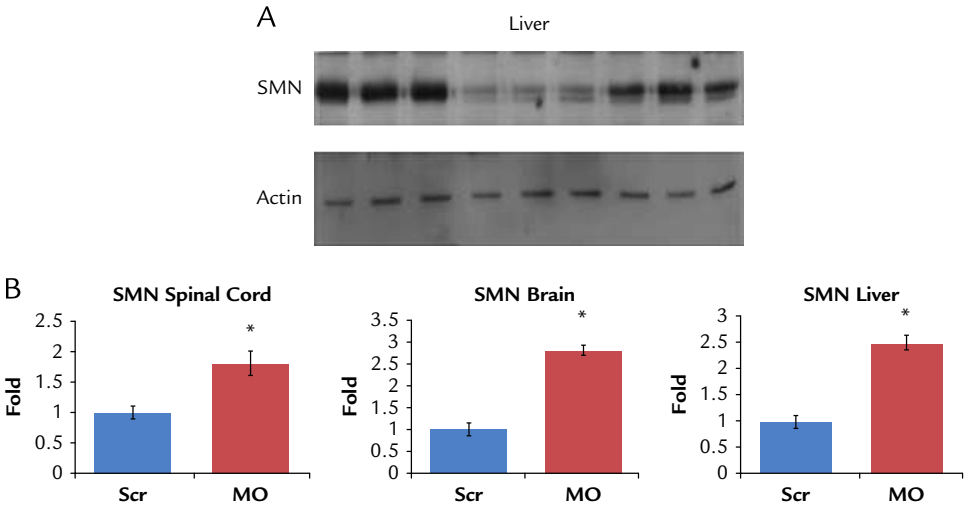

Supplemental Figure 2. Morpholino oligomer (MO) 10 to 34 (MO-10-34) treatment increases SMN protein level in spinal muscular atrophy (SMA) mice. Treatment with MO-10-34 increased SMN protein expression after intracerebroventricular and subcutaneous injection of neonatal mice with severe SMA at posnatal days 0 and 3. (A) Seven days after treatment, the amount of SMN protein in the liver of MO-10-34–treated mice relative to scramble (Scr)–treated and wild-type mice was evaluated by Western blotting, indicating a significant increase in SMN. (B) The densitometric analysis revealed that the amount of SMN protein in the spinal cord, brain, and liver of MO-10-34–treated mice relative to Scr-treated and wild-type mice evaluated by Western blotting was significantly increased. *$P < 0.001$.

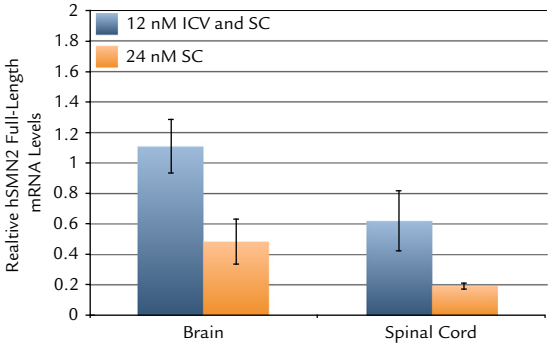

Supplemental Figure 3. Morpholino oligomer (MO) 10 to 34 (MO-10-34) combined treatment increases SMN levels in the central nervous system more efficiently with respect to only subcutaneous (SC) treatment. Human SMN2 (hSMN2) full-length mRNA levels increased significantly in the combined administration compared with SC administration only (brain, 2.29-fold; $P = 0.026$; spinal cord, 3.26-fold; $P = 0.048$). hSMN2 full-length mRNA levels are shown relative to intracerebroventricular (ICV) and SC treated samples and normalized to 5.8S rRNA. Data are mean (SEM).

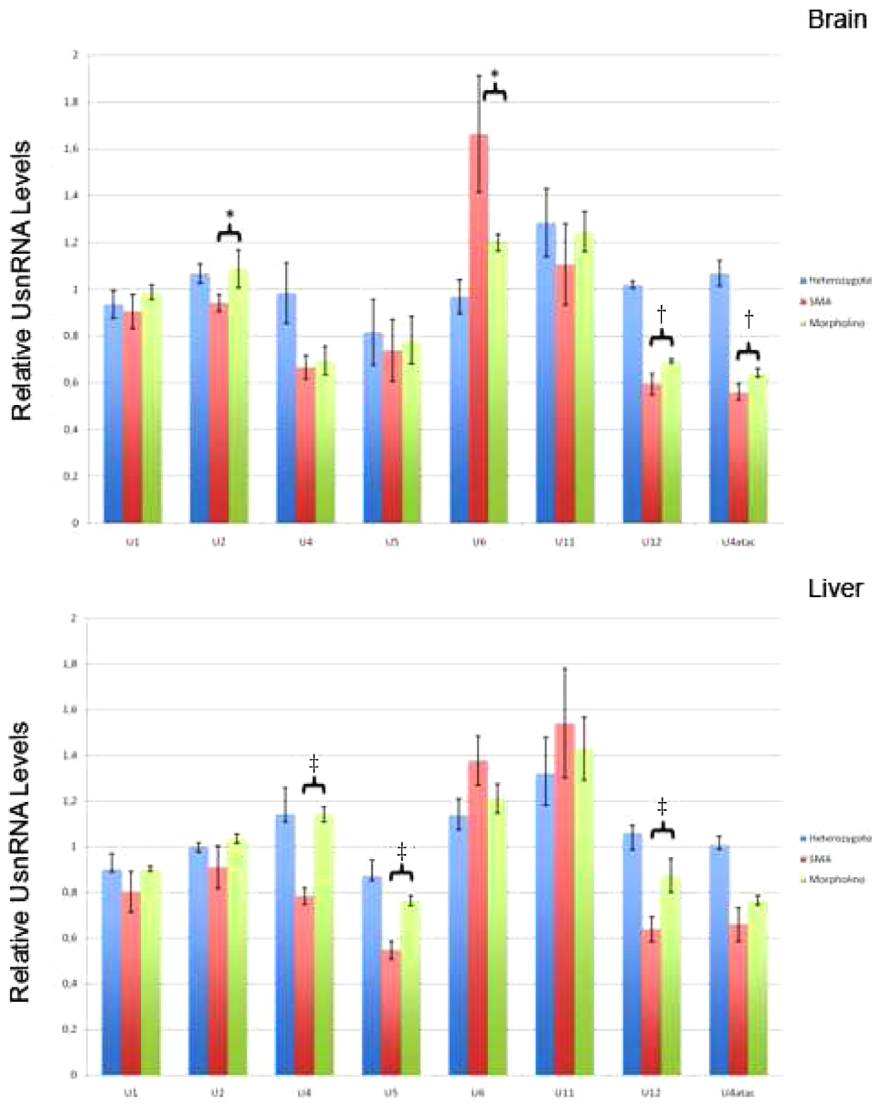

Supplemental Figure 4. Morpholino oligomer (MO) 10 to 34 (MO-10-34) treatment restores the small nuclear RNA (snRNA) expression levels that were deregulated in spinal muscular atrophy (SMA) mice. snRNA expression levels are deregulated in SMA mice and partially restored after MO treatment. Data are mean (SEM). The uridylate-rich snRNA (UsnRNA) levels are normalized to 7SL-RNA and set relative to the levels in the heterozygous (Het) mice. Scr = scramble. *$P < 0.1$, †$P = 0.05$, ‡$P < 0.01$.

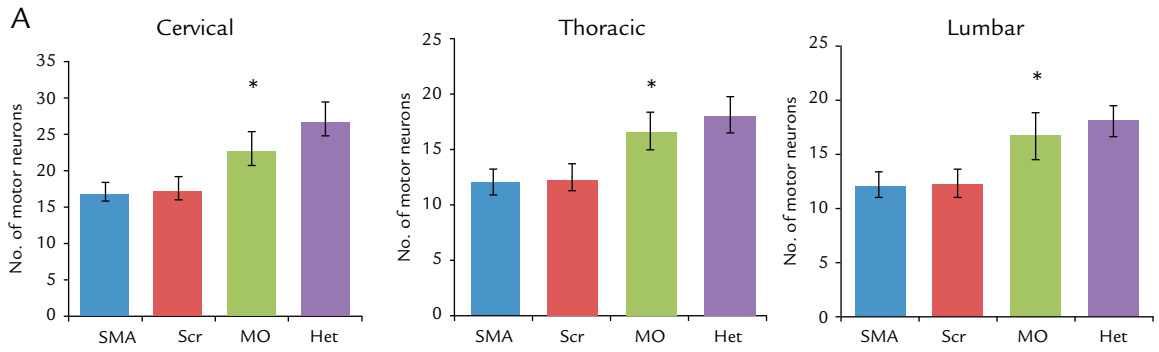

Supplemental Figure 5. Morpholino oligomer (MO) treatment increased the number of spinal cord motor neurons. Neuropathologic analysis demonstrated an increase in motor neuron number in the spinal cord after intracerebroventricular and subcutaneous injection of neonatal spinal muscular atrophy (SMA) mice at postnatal day 0 (P0) and P3. The number of motor neurons in the cervical, thoracic, and lumbar regions was determined by ChAT immunostaining at 9 days. Data are mean (SEM). *P* values between different treatment groups were determined using 1-way ANOVA and Bonferroni multiple post hoc comparisons ($P < 0.001$). Het = heterozygous; Scr = scramble.

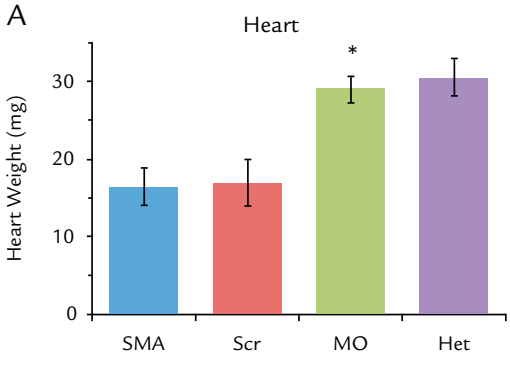

Supplemental Figure 6. Morpholino oligomer (MO) treatment improved heart trophism in spinal muscular atrophy (SMA) mice. Heart weight significantly improved in MO-treated mice vs scramble (Scr)–treated mice ($P < 0.001$). *P* values between different treatment groups were determined using 1-way ANOVA and Bonferroni multiple post hoc comparisons ($P < 0.001$). Het = heterozygous.

Supplemental Table I. Oligo sequences used for mRNA analyses. f ¼ ; F ¼ ; Q12 FL ¼ full length; hSMN2 ¼ human SMN2; R ¼; RT ¼ reverse transcription; TOT ¼ total; qPCR ¼ quantitative polymerase chain reaction; snRNA ¼ small nuclear RNA.

snRNA Analysis	Oligo name	Sequence 5′-3′
	small RNA RT primer	GCTGTCAACGATACGCTACGTAACGGCATGACAGTG-TTTTTTTTTTTTTTTTVN
	small RNA reverse	GCTGTCAACGATACGCTACGTAAC
	mm qPCR f U1	TTCGCGCTCTCCCCTGAA
	mm qPCR f U2	CAGGAACGGTGCACCAA
	mm qPCR f U4	GACAGTCTCTACGGAGACTGAA
	mm qPCR f U4atac	ACC TTG GTG CAA TTT TTG GAA AAA A
	mm qPCR f U6	TCGTGAAGCGTTCCATATTTTTAA
	7SL qPCR f	CCTGGGCAACATAGCGAGAC
mRNA Analysis	**Oligo name**	**Sequence 5′-3′**
	hSMN2-FL F	CACCACCTCCCATATGTCCAGATT
	hSMN2-FL R	GAATGTGAGCACCTTCCTTCTTT
	hSMN2-TOT F	GTGAGGCGTATGTGGCAAAAT
	hSMN2-TOT R	CATATAGAAGATAGAAAAAAACAGTACAATGACC
	mm Gapdh F	AATGTGTCCGTCGTGGATCTGA
	mm Gapdh R	GATGCCTGCTTCACCACCTTCT

Oligo sequences used for mRNA analyses. f = forward; F = forward; FL = full length; hSMN2 = human SMN2; R = reverse; RT = reverse transcription; TOT = total; qPCR = quantitative polymerase chain reaction; snRNA = small nuclear RNA.